# **Theoretical Microfluidics**

MICRO-718

T. Lehnert and M.A.M. Gijs (EPFL-LMIS2)

EPFL - Lausanne
Doctoral Program in Microsystems and
Microelectronics (EDMI)







# 4. Diffusion and mixing in microscale

- 4.1 Diffusion: Principles and applications
- 4.2 Fast mixing in microscale

"Microfluidics" -- Thomas Lehnert -- EPFL (Lausanne)

# **EPFL**

# 4.1 Diffusion: Principles and applications

- 4.1.1 Molecular diffusion: Fast or slow?
- 4.1.2 The passive scalar transport equation
- 4.1.3 The diffusion equation
- 4.1.4 Diffusion-based microfluidic devices

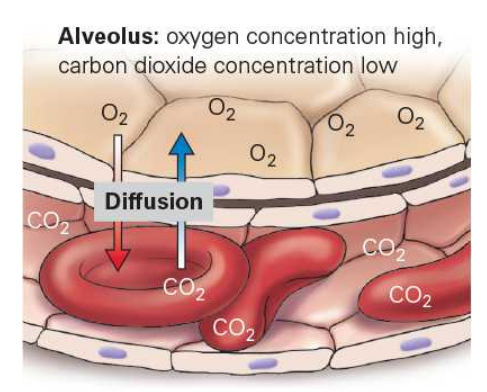
# 4.1.1 Molecular diffusion: Fast or slow?

**EPFL** 

**Molecular diffusion**: A substance tends to move from a region of high concentration to a region of low concentration until its concentration becomes equal throughout a space.

The microscopic explanation for diffusion is based on kinetic theory and the random motion of molecules (Brownian motion).

Molecular/ionic transport by diffusion is fundamental to natural processes.



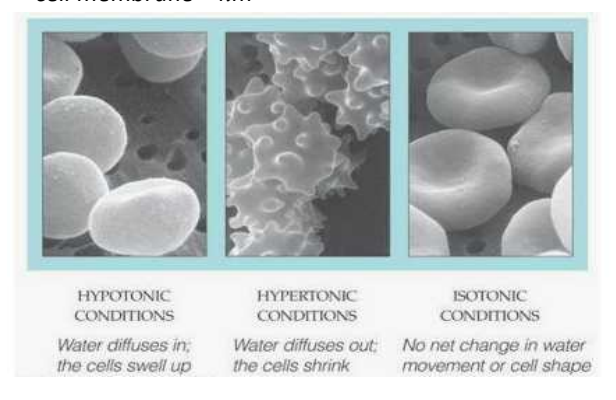
Capillary: oxygen concentration low, carbon dioxide concentration high

Receptor

Synapse

synaptic cleft ≈ 20 - 40 nm

Osmosis (red blood cells) *cell membrane* ≈ *nm* 



"Microfluidics" -- Thomas Lehnert -- EPFL (Lausanne)

# **EPFL**

Thermodynamic description of diffusion

The Gibbs free G energy including the chemical potential  $\mu_i$  is given by:

$$\mathrm{d}G = -S\,\mathrm{d}T + V\,\mathrm{d}P \, + \sum_{i=1}^n \mu_i \mathrm{d}N_i$$

$$\mu_i = \left(rac{\partial G}{\partial N_i}
ight)_{T,P,N_{j
eq i}}$$

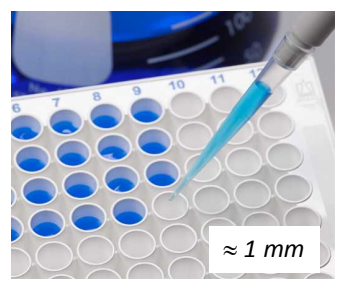
Particles tend to move from higher chemical potential  $\mu_i$  to lower chemical potential: Driving force  $\sim (-\nabla \mu_i)$  or  $\sim (-\nabla c_i)$ .

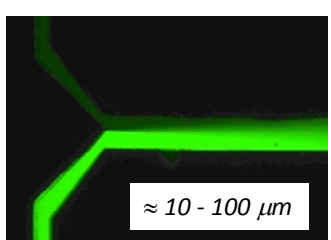


$$L_0 = \sqrt{DT_0} \qquad \text{or} \qquad T_0 = \frac{L_0^2}{D}$$

D Diffusion coefficient,  $L_{\boldsymbol{\theta}}$  diffusion length,  $T_{\boldsymbol{\theta}}$  diffusion time

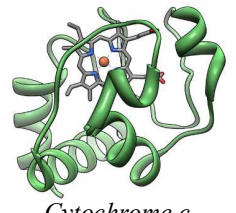






# Diffusion constants and diffusion times







\_\_ Flu virus

Characteristic diffusivities				
Particle	Typical size	Diffusion constant	$T_{\theta}$ (100 $\mu$ m)	$T_0$
Solute ion	$10^{-1} \text{ nm}$	$2 \times 10^3 \ \mu \text{m}^2/\text{s}$	5s	
Small protein	5 nm	$40 \ \mu \text{m}^2/\text{s}$	≈ 4 min	
Virus	100 nm	$2 \mu \text{m}^2/\text{s}$	≈ 1h 20 min	
Bacterium	$1 \mu m$	$0.2 \ \mu m^2/s$	> 2 days	
Mammalian/human cell	10 μm	0.02 μm <sup>2</sup> /s	> 20 days	

T.M. Squires et al., Rev. Mod. Phys., Vol. 77, p. 977, 2005

#### Diffusion time $T_0$ across a typical microchannel (width 100 µm)

Another example: Diffusion of a fluorescent dye (fluorescein,  $D=3 \times 10^{-6} \text{ cm}^2/\text{s}$ ) in a glass of water  $T_0 > 400 \text{ days}$  ( $L_0=10 \text{ cm}$ ) - in microchannel  $T_0 \approx 300 \text{ ms}$  ( $L_0=100 \text{ }\mu\text{m}$ ).

"Microfluidics" -- Thomas Lehnert -- EPFL (Lausanne)

# **EPFL**

# Einstein relation for diffusion

A. Einstein (Annalen der Physik, 1905), doi.org/10.1002/andp.19053220806

Einstein analyzed the random motion of a **spherical particle** suspended in a solution and hypothesized that it is identical to Brownian motion. He raised the question to which extend classical thermodynamics is valid on the microscopic scale.

- Diffusion flow density J

$$\mathbf{J} = -D \, \boldsymbol{\nabla} \rho$$

- Force driving diffusion (chem. potential  $\mu$ )

$$\mathbf{F}_{\text{diff}} = -\nabla \mu \tag{6.48}$$

- Force balance using Stokes drag force

$$\mathbf{F}_{\text{drag}} = \mathbf{F}_{\text{diff}}$$

- and with (solute density  $\rho$ , bulk solution density  $\rho_0$ )

$$\mu = \mu_0 + kT \ln(\rho/\rho_0)$$

(see Appendix D in H. Bruus)

 $\Rightarrow$  Einstein relation for the diffusion coefficient  $D(T, \eta)$  in liquids

$$D = \frac{k_{\rm B}T}{6\pi a\eta}$$

(6.49)

(assuming a drag force in the Stokes regime, temperature T, radius a, dynamic viscosity  $\eta$ )

Möge es bald einem Forscher gelingen, die hier aufgeworfene, für die Theorie der Wärme wichtige Frage zu entscheiden!

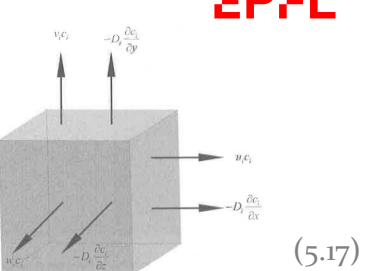
Bern, Mai 1905.

# 4.1.2 The passive scalar transport equation

**EPFL** 

The transport of a solute  $\alpha$  (density  $\rho_{\alpha}$ ) in a heterogeneous solution is determined by the convection field  $\mathbf{v}(\mathbf{r},t)$  of the solution and diffusion relative to the bulk solution (total density  $\rho$ ). The mass current density  $\mathbf{J}_{\alpha}$  for the solute  $\alpha$  can be written as (with  $c_{\alpha} \equiv \rho_{\alpha}/\rho$ ):

$$\mathbf{J}_{\alpha} \equiv \mathbf{J}_{\alpha}^{\mathrm{conv}} + \mathbf{J}_{\alpha}^{\mathrm{diff}} = \rho_{\alpha}\mathbf{v} + \mathbf{J}_{\alpha}^{\mathrm{diff}} = c_{\alpha}\rho\mathbf{v} + \mathbf{J}_{\alpha}^{\mathrm{diff}}$$



**Mass continuity equation** for a solute density  $c_{\alpha}\rho$ : Diffusion appears as flow through the surface  $\partial\Omega$ 

$$\int_{\Omega} d\mathbf{r} \, \partial_t (c_{\alpha} \rho) = -\int_{\partial \Omega} da \, \mathbf{n} \cdot \left( c_{\alpha} \rho \mathbf{v}(\mathbf{r}, t) + \mathbf{J}_{\alpha}^{\text{diff}} \right) = -\int_{\Omega} d\mathbf{r} \, \nabla \cdot \left( c_{\alpha} \rho \mathbf{v}(\mathbf{r}, t) + \mathbf{J}_{\alpha}^{\text{diff}} \right)$$
(5.18)

reduces to 
$$(\rho = \text{const}, \text{div } \mathbf{v} = 0)$$
 
$$\rho \left[ \partial_t c_\alpha + \mathbf{v} \cdot \nabla c_\alpha \right] = -\nabla \cdot \mathbf{J}_\alpha^{\text{diff}}$$
 (5.20)

with Fick's 1st law (for small gradients)

$$\mathbf{J}_{\alpha}^{\text{diff}} = -D_{\alpha} \,\rho \,\boldsymbol{\nabla} c_{\alpha} \tag{5.21}$$

 $D_{\alpha}$  is the diffusion constant of a solute  $\alpha$  [m<sup>2</sup>/s]

⇒ Convection - diffusion eqn (a scalar conservation eqn)

$$\partial_t c_\alpha + \mathbf{v} \cdot \nabla c_\alpha = D_\alpha \, \nabla^2 c_\alpha \tag{5.22}$$

 $c_{\alpha}$  can be replaced by  $c^{*}_{\ \alpha}$  =  $N_{\alpha}/V$  (number of molecules/volume)

# 4.1.3 The diffusion equation



Without convection ( $\mathbf{v} = 0$ ) eqn (5.22) becomes (for a single solvent,  $\alpha$  is suppressed)

Mass diffusion equation (2nd Fick's law)

$$\partial_t c = D \ \nabla^2 c \tag{5.26}$$

Dimensional analysis reveals characteristic length and time scales over which  $c(\mathbf{r},t)$  varies:

$$L_0 = \sqrt{DT_0}$$
 or  $T_0 = \frac{L_0^2}{D}$  (5.27)

A momentum diffusion equation with the kinematic viscosity  $\nu$  as diffusion coefficient was derived earlier from the transient Stokes eqn (see chapter 2.5):

$$\partial_t(\rho v_x) = \nu \nabla^2(\rho v_x)$$
  $\nu \equiv \frac{\eta}{\rho} \quad (\approx 10^{-6} \text{ m}^2/\text{s for water})$  (5.43)

A dimensionless number describing intrinsic diffusive properties of a fluid can be defined as:

$$Sc = \text{Schmidt number} \equiv \frac{\nu}{D} = \frac{\eta}{\rho D}$$
 (5.46)

# Solutions of the mass diffusion equation



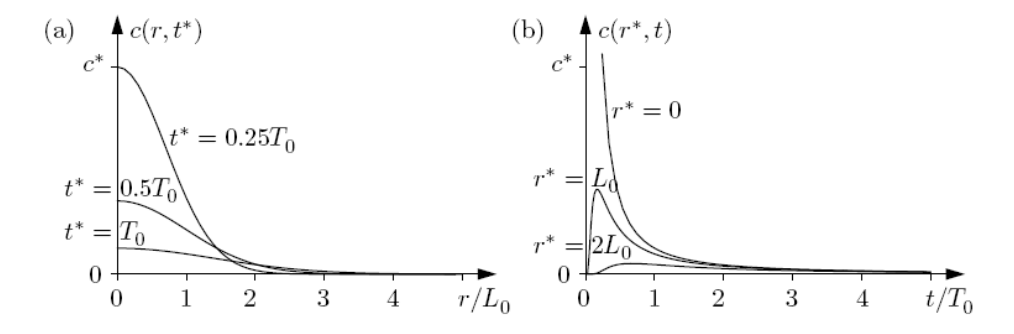
#### 1) Limited point-source diffusion

A fixed number of ink molecules is injected in a solution at  $\mathbf{r} = 0$  and t = 0:

$$c(\mathbf{r},t=0) = N_0 \, \delta(\mathbf{r}) \quad \xrightarrow{in \, (5.26)} \quad c(\mathbf{r},t>0) = \frac{N_0}{(4\pi Dt)^{\frac{3}{2}}} \, \exp\left(-\frac{r^2}{4Dt}\right) \tag{5.35}$$

(for 3D, normal distributions in x,y,z)

 $l_{\text{diff,1D}}^2 = 2 Dt$   $l_{\text{diff,2D}}^2 = 4 Dt$   $l_{\text{diff,3D}}^2 = 6 Dt$ The diffusion length  $l_{diff}$  is determined by the variance of (5.35) and increases with dimension (1D, 2D or 3D).



3D concentration  $c(\mathbf{r},t>0)$  for three different  $t^*$  and  $\mathbf{r}^*$  values, respectively.  $L_0$  and  $T_0$  are (Fig. 5.2) characteristic length and time scales.

# EPFL

# 2) Constant planar-source diffusion

For t > 0 constant concentration of solute at x = 0, solute influx through the boundary plane:

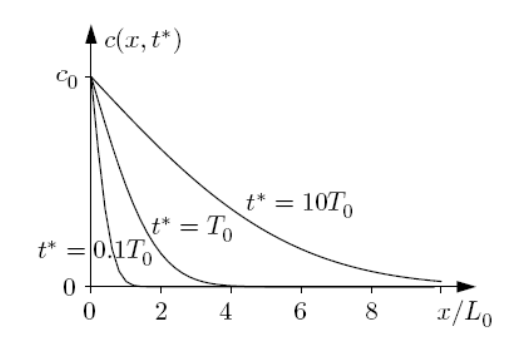
$$c(x = 0, y, z, t > 0) = c_0$$

(Fig. 5.3)

$$c(\mathbf{r},t>0) = c_0 \operatorname{erfc}\left(\frac{x}{\sqrt{4Dt}}\right) \qquad \textit{with} \qquad \qquad \operatorname{erfc}(s) \equiv \frac{2}{\sqrt{\pi}} \, \int_s^\infty e^{-u^2} \, \mathrm{d}u$$

$$\mathrm{erfc}(s) \equiv \frac{2}{\sqrt{\pi}} \, \int_s^\infty e^{-u^2} \, \mathrm{d}u \qquad (5.41)$$

Complementary error function



Microchannel Diffusion 1D

Concentration c(x,t>0) for different  $t^*$  values.

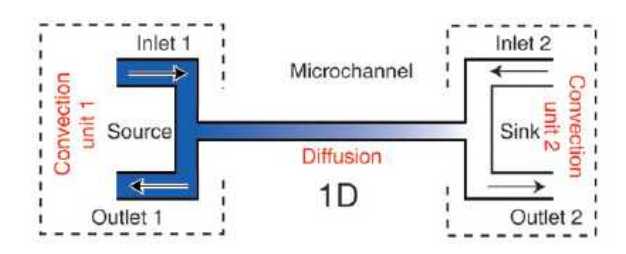
Microfluidic configuration for a constant planar source. J. Atencia et al., Lab Chip, 2009, 9, 2707-2714

#### 4.1.4 Diffusion-based microfluidic devices



# Example 1: A microfluidic concept to generate constant diffusion profiles

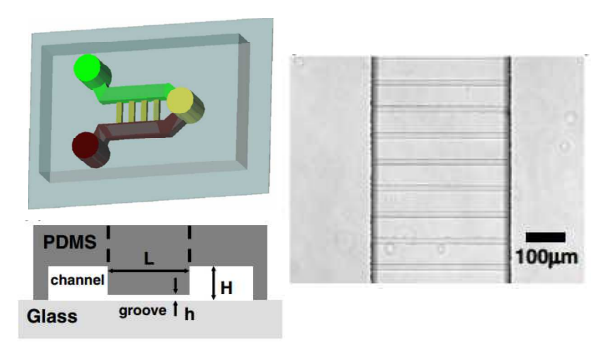
W. Saasi et al., Biomedical Microdevices, Vol. 9, pp 627-635 (2007)

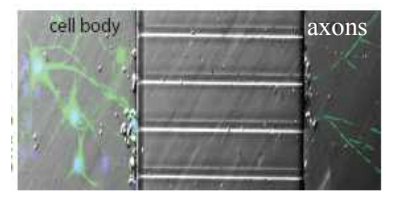


- $\Rightarrow$  Convection units 1 and 2 act as a perfect source or sink ( $c_{source}$  and  $c_{sink}$  are const.), respectively (the analyte is replenished/removed permanently.
- ⇒ No pressure drop on microchannel, mass transfer only through diffusion.

J. Atencia et al., Lab Chip, 2009, 9, 2707-2714

Microfluidic "ladder" geometry: Main channel height 100  $\mu$ m, lateral groove height 5  $\mu$ m):  $R_{groove} << R_{main}$ 





Possible application: gradients of growth factors for axon growth through the microchannels.

#### Concentration gradient generation in the microgrooves:

Fluorescence intensity profile across a microgroove as a fct. of time. Right and left inlets loaded with FITC-dextran and PBS, respectively.

$$C(x,t) = \sum_{n} \left\{ \frac{2Ln\pi (C_0 - C_L - C_0(-1)^n + C_R(-1)^n)}{Ln^2\pi^2} \right.$$

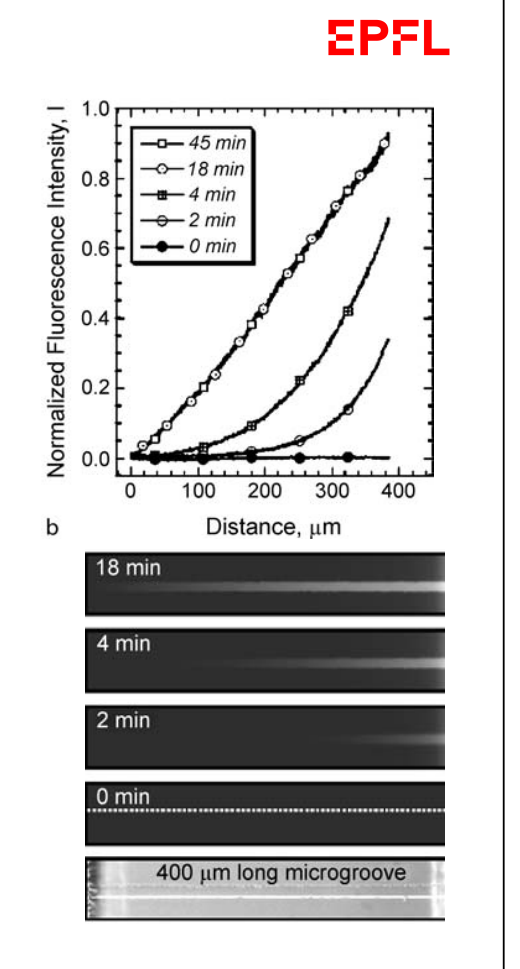
$$\times sin\left(\frac{n\pi x}{L}\right) e^{-D\left(\frac{n\pi}{L}\right)^2 t} \left. \right\} + \frac{C_R - C_L}{L} x + C_L$$
for t >> 0
$$C = \frac{C_R - C_L}{L} x + C_L,$$

⇒ A linear steady-state gradient was established after 18 min.

#### Application:

Cell-based chemotaxis assays (no shear forces !), *e.g.* neutrophils (white blood cells) migrating in a linear IL-8 chemokine gradient. IL-8 is a signaling protein causing the cells to migrate toward the site of infection.

W. Saasi et al., Biomedical Microdevices, Vol. 9, pp 627-635 (2007)



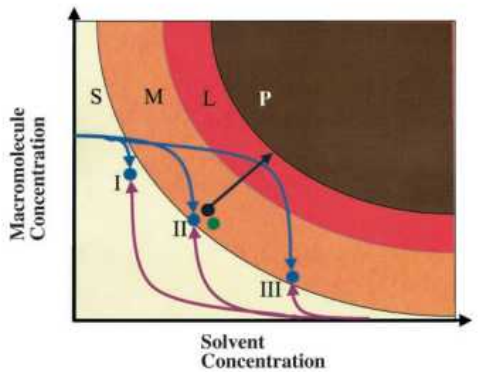
#### Example 2: Protein crystallisation in microfluidic chambers

In 1958, the 3D structure of myoglobin was determined by X-ray crystallography.

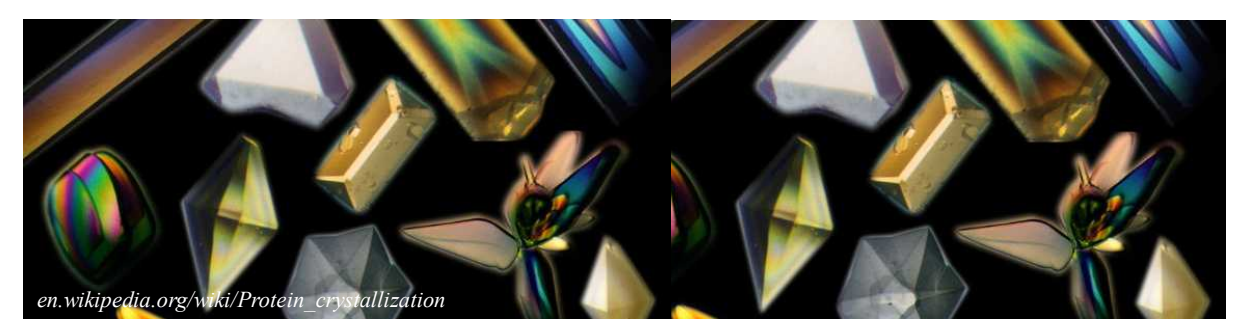
Determination of appropriate crystallization conditions of these marcomolecules is difficult!

#### Important parameters:

- **Protein solution** (purity and concentration)
- pH (**buffers** such as Tris-HCl)
- **Precipitants** (*e.g.* ammonium sulfate or polyethylene glycol/PEG), and additives
- Temperature



C. Hansen, et. al, PNAS 2002, 99: 16531-16536



#### Problems in conventional approches

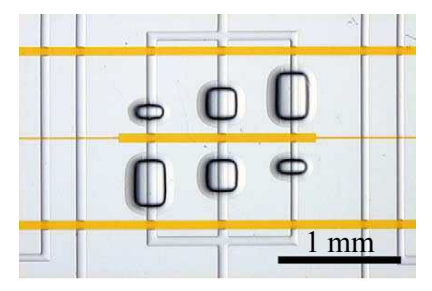
- Entirely empirical process, manual or automated pipetting (hundreds of solutions to be tested).
- Available quantity / cost of purified proteins samples (sometimes only sub-milligram)
- Fluidic/local chemical conditions not well-defined.
- Difficulty in dispensing small volumes of some highly viscous solutions used in crystallography.

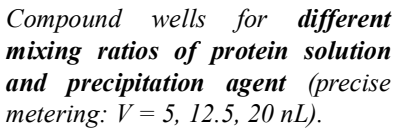
#### Advantages of micrcofluidic solution

- Highly parallel approach (here 144 reactions)
- Very low sample volume (nL range)
- Precice metering
- Unique diffusive mixing dynamics!

# Protein Solution Glass Cover Slide Protein Solution and Precipitant Vacuum Grease Hanging droplet method Solution Integrated PDMS device

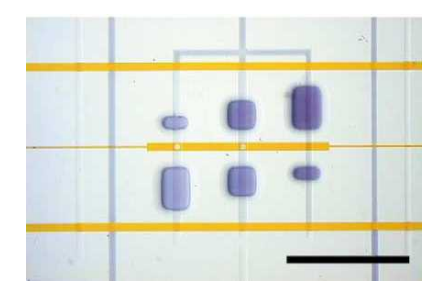
Detail of the PDMS/glass chip: 3 pairs of reaction chambers separted by valves.







"Dead-end" sample loading of gas permeable PDMS chambers (middle control line closed, bottom line open).



Interface valves open (middle control line open, others closed): Diffusion and reaction.

- Ideally stable fluidic conditions and unique kinetics: "Free interface diffusion".
- No convection due to densities variations: viscous force high compared to buoyant force.
- The high chemical gradient is localized in the channel in between the chambers.
- Kinetics of equilibration: Solvents diffuse "fast" (< 1 h), proteins "slow" (8 to 24 h to equilibrium).
  - C. Hansen, et. al, PNAS 2002, 99: 16531-16536
- C. Hansen and S. Quake, Current Opinion in Structural Biology 2003, 13:538-544

**EPFL** 

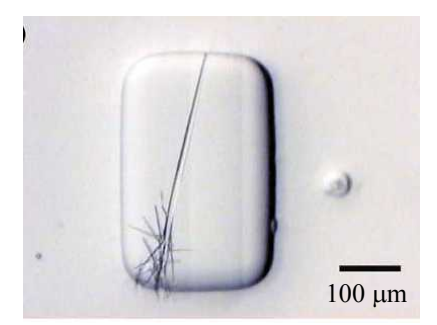
Crystal of the catalytic core domain of bacterial *primase*.

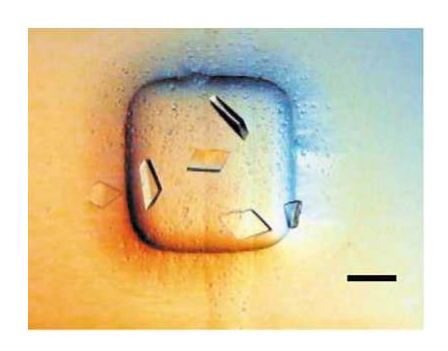
Function: Catalyzes the synthesis of a short RNA primer complementary to a ssDNA template for DNA replication by DNA polymerases.

Large single crystals of a type II *topoisomerase ATPase* domain bound to ADP.

Function: Cut both strands of a DNA helix

Growth time is less than 12 hours on a chip (more than 1 week of incubation in conventional setup).





C. Hansen and S. Quake Current Opinion in Structural Biology 2003, 13:538–544

# 4.2 Fast mixing in microscale

- 4.2.1 Microfluidic mixing concepts
- 4.2.2 Diffusion mixing vs. convection (Péclet number)
- 4.2.3 Enhancing diffusion mixing by flow lamination
- 4.2.4 Taylor dispersion and the rotary mixer
- 4.2.5 A multivortex mixer based on inertial flow properties
- 4.2.6 Chaotic mixing in microchannels

"Microfluidics" -- Thomas Lehnert -- EPFL (Lausanne)

# 4.2.1 Microfluidic mixing concepts

# **EPFL**

#### Marcoscale mixers

Stirring at high Re numbers, inertial flow properties, turbulent mixing.

#### Microscale mixers

Applications: On-chip chemical reactors (mixing should be faster than reaction kinetics, bioassays require homogenous distribution of reagents, etc.). Small internal volumes of chip-based mixers may be an advantage, *i.e.* with respect to hazardous chemical reactions or precious samples biological analysis.

#### Problems related to mixing in microscale (miscible liquids):

- ⇒ At low *Re* numbers flow is laminar, deterministic and reversible.
- ⇒ No hydrodynamic instabilities (*e.g.* wakes). Simple flow perturbations do not promote efficient mixing (*e.g.* obstacles in channel).
- ⇒ Diffusion over the channel width is a generally too slow (especially for larger biomolecules).



Laminar flow around «obstacles» (bubbles)



#### The final stage of all mixing concepts is molecular diffusion!

'The art of micromixing' translates into the efficient maximization of interfacial surface areas and reducing the molecular diffusion length by generating high local concentration gradients.

**Active mixing** by time-pulsing flow owing to a periodical change of pumping energy or electrical fields, acoustic fluid shaking, ultrasound, electrowetting-based droplet shaking, microstirrers, and others.

**Passive mixing (no moving parts)** in split-and-recombine flow cells, by multi-laminating and chaotic advection, by recirculation of secondary flows, jet colliding, and others.

#### Some references:

Nguyen NT. (2007) Mixing in Microscale. In: Hardt S., Schönfeld F. (eds) Microfluidic Technologies for Miniaturized Analysis Systems. Springer, Boston, MA - doi.org/10.1007/978-0-387-68424-6 3

G.S. Jeong et al., Applications of micromixing technology, Analyst, 2010, 135, 460–473

Y. K. Suh et al., A Review on Mixing in Microfluidics, Micromachines 2010, 1, 82-111

C.-Y. Lee et al., Passive mixers in microfluidic systems: A review, Chemical Eng. Journal, 288 (2016) 146-160

C.-Y. Lee et al., Recent advances and applications of micromixers, Sensors and Actuators B 259 (2018) 677–702

"Microfluidics" -- Thomas Lehnert -- EPFL (Lausanne)

Possible **passive approaches** to generate high local gradients in the low *Re* number range are:

- Flow focusing
- Parallel or serial lamination of different species
- Rotary mixers competing Taylor-Aris dispersion (band broadening)
- Splitting and folding the flow (Chaotic advection)

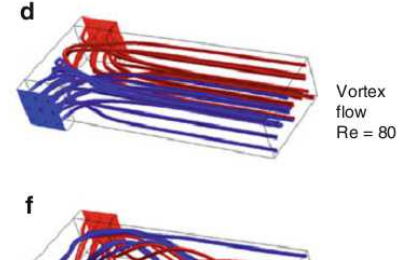


Stiration in laminar flow regime

Micromixers designed for higher *Re* numbers may take advantage of emerging inertial/turbulent effects, such as:

- Wake formation (boundary separation at channel extensions)
- Dean flow vortice
- Other flow instabilities

High Re numbers are inconvenient in microscale (high pressure, flow speeds up to  $\approx m/s$ ).





T-junction: Transition from laminar to swirling/turbulent flow.



# 4.2.2 Diffusion mixing vs. convection (Péclet number)

Convective and diffusive transport in a fluidic system may be compared by a dimensional analysis of the convection-diffusion equation (5.22), and by introducting a parameter *Pe*.

$$Pe \,\partial_{\tilde{t}}c + Pe \,\frac{a}{L_0} \,\tilde{v}_x \partial_{\tilde{x}}c = \left(\partial_{\tilde{r}}^2 c + \frac{1}{\tilde{r}} \,\partial_{\tilde{r}}c\right) + \frac{a^2}{L_0^2} \,\partial_{\tilde{x}}^2 c. \tag{5.52}$$

convection radial diffusion axial diffusion

(eqn 5.22 in cylinder coordinates, flow in x-direction in a tube with radius a, flow speed  $V_0$ ):

$$Pe \equiv \frac{\text{diffusion time}}{\text{convection time}} = \frac{\tau_{\text{diff}}^{\text{rad}}}{\tau_{\text{conv}}^{a}} = \frac{\frac{a^{2}}{D}}{\frac{a}{V_{0}}} = \frac{V_{0} a}{D} \quad (dimensionless) \quad (5.53)$$

The **Péclet number** Pe indicates the relative importance of diffusive and convective mass transport by comparing the time  $\tau$  required to move over a typical length scale of the device (e.g. the tube radius a).

$$\tau_{\rm diff}^{\rm rad} = \frac{a^2}{D},$$
 time to move the distance  $a$  by radial diffusion 
$$\tau_{\rm conv}^a = \frac{a}{V_0},$$
 time to move the distance  $a$  by axial convection (5.51)

For high Pe numbers convection dominates ( $\tau^a_{conv} << \tau^{rad}_{diff}$ ), for low Pe numbers diffusion dominates ( $\tau^{rad}_{diff} << \tau^a_{conv}$ ). Pe numbers may vary over a wide range in microsystems ( $\approx 10^{-2}$  to  $10^{5}$ ).

 $"Microfluidics" -- Thomas\ Lehnert -- EPFL\ (Lausanne)$ 

# **EPFL**

# Evaluation of the Péclet number in a straight channel

*Example:* Two equal solutions are combined in a Y-junction, one contains small proteins (laminar flow regime, flow velocity  $V_0$ , the channel width w).

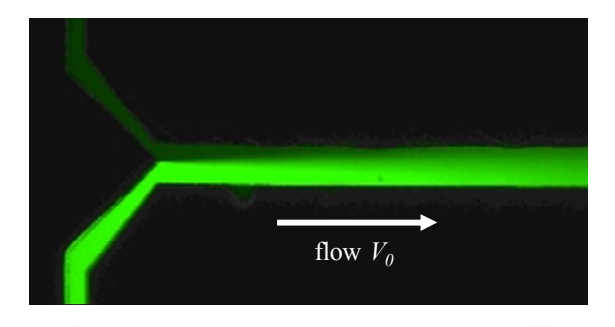
$$D \approx 50 \ \mu \text{m}^2/\text{s}$$
 ;  $V_0 = 50 \ \mu \text{m/s}$  ;  $w = 100 \ \mu \text{m}$ 

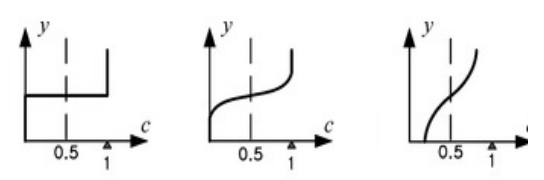
How far down the channel  $(l_{mix})$  full diffusive mixing will have occurred (*i.e.* the protein concentration is uniform over the channel width)?

$$l_{mix} = \tau_{diff} \cdot V_0$$
 with  $\tau_{diff} = w^2/D$   
 $\tau_{diff} = 200 \text{ s} \approx 3 \text{ min} \Rightarrow l_{mix} \approx 1 \text{ cm} \approx 100 \cdot w$ 

$$Pe = V_0 w/D = l_{mix}/w \Rightarrow Pe = 100$$

The *Pe* number can be written as the ratio of mixing length to the dimension of lateral diffusion. The diffusive profile across a channel at a given location depends on the *Pe* number.





Concentration distribution in a microchannel. The graphs show the concentration distribution normal to the channel wall (*y*) at several channel sections.

Y.K. Suh et al., Micromachines 2010, 1(3), 82-111

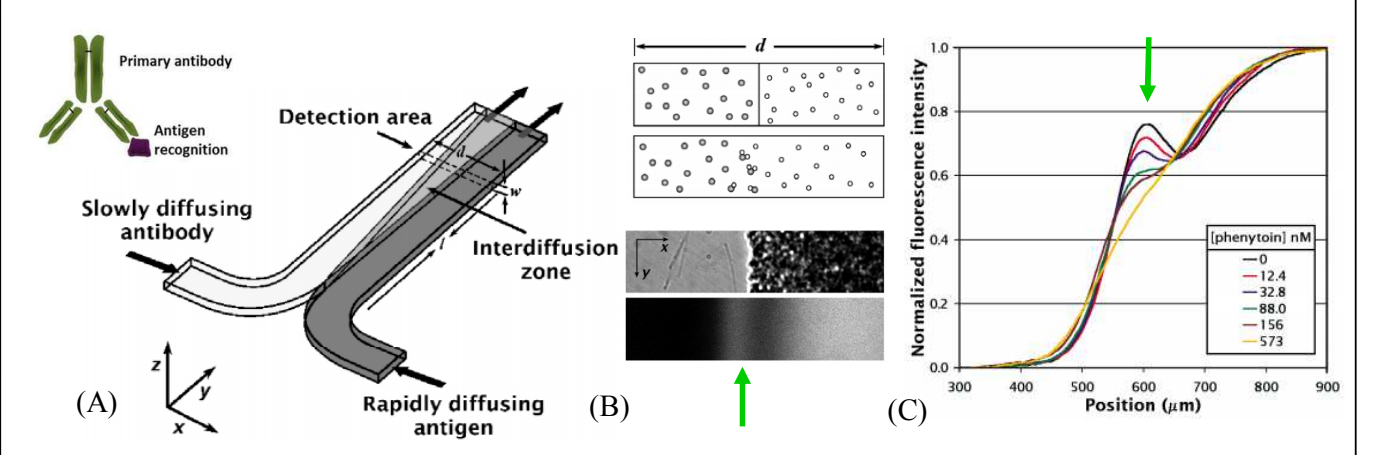
## Example 1: A rapid diffusion immunoassay in a T-sensor



A. Hatch et al., Nature biotechnology, vol. 19 (2001), 461-465

Competitive immunoassay measuring the distribution of a fluorescently labeled probe molecule (antigen) at a fixed location after diffusion into a region containing antigen-specific antibodies.

Clinically relevant levels of phenytoin (a small-sized antiepileptic drug molecule) were measured (nM range, < 1 min). Removal of cells from blood samples was not necessary.



(A) T-Sensor and detection area; (B) The presence of slowly diffusing Ab limits the diffusive transport of antigen, causing it to accumulate in the center of the channel. Bright-field image of blood solution spiked with labeled antigen and fluorescence image. (C) Modified antigen diffusion profile for different concentrations. The competitive assay (labelled + sample antigens) generates the strongest signal at lowest sample antigen concentrations.

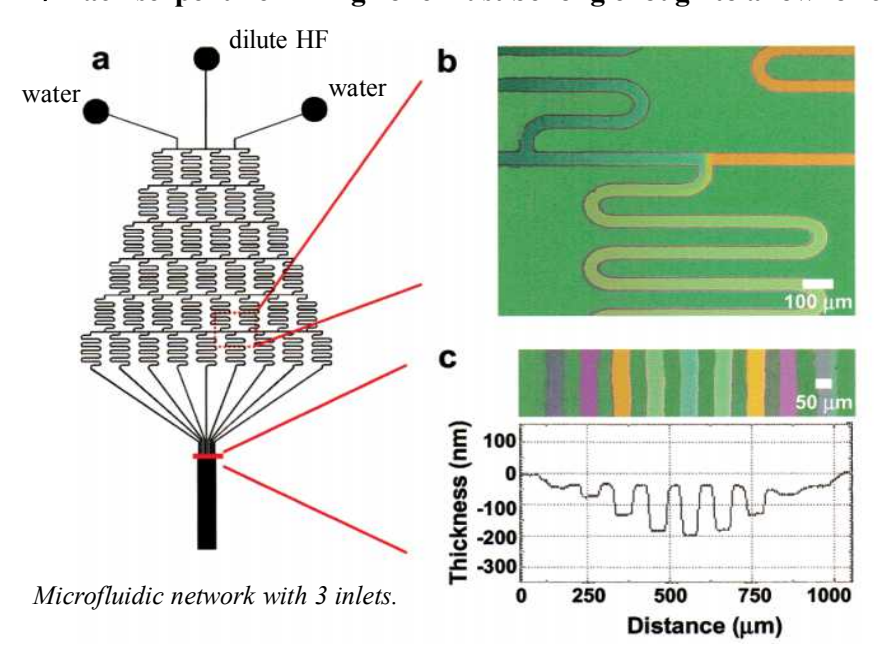
# Example 2: Concentration gradient generator (CGG)



N.L. Jeon, Langmuir 2000, 16, 8311-8316

Microfluidic network based on the controlled diffusive mixing of laminar flow fluids by repeated splitting, mixing, and recombination network.

#### ⇒ Each serpentine mixing zone must be long enough to allow for complete diffusive mixing.



A HF concentration gradient is used to generate a gradient in topology in a 500 nm thick SiO<sub>2</sub> layer on a Si wafer.

Differences in the thickness of the  $SiO_2$  layer give rise to the different interference colors in the etched channels.

Oxide color observation and surface profilometer scan across separate channels immediately before combining them into a single large channel.

Further information (review paper): A.G.G. Toh et al., Microfluid Nanofluid (2014) 16:1–18

# 4.2.3 Enhancing diffusion mixing by flow lamination

## Example 1: Diffusive mixing enhanced by hydrodynamic flow focusing

J. Knight et al., Phys. Rev. Lett. Vol 80 (17), pp. 3863-3866 (1998)

- Flow lamination and focusing of a central stream in between two sheath flows.
- Molecules diffuse rapidly across the central stream.

#### Ultrathin hydrodynamic focusing

 $\Rightarrow$  Relevant mixing time constant:  $\tau$ 

 $\tau_{mix} = w^2/D$ 

⇒ Focusing width

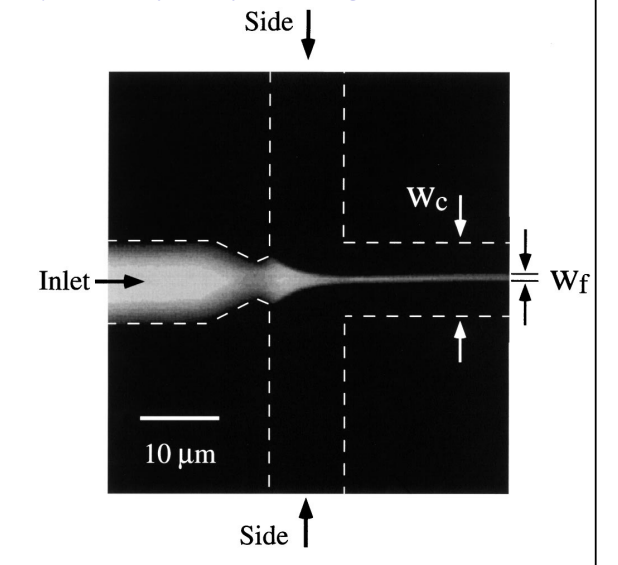
 $w_f < 50 \text{ nm}$ 

⇒ Diffusive mixing time

 $\tau_{mix} < 10 \ \mu s$ 

Example application: Resolving fast protein folding, e.g. Cytochrome c ( $\tau_{folding} = 400 \mu s$ ) by changing pH in the injected sample solution ( $Cyt\ c$  is a component of the electron transport chain in mitochondria).

L. Pollack et al. PNAS, Vol 96, pp. 10115 (1999)



Hydrodynamic focusing on a Si/glass chip: The channels are outlined with a dashed line (10  $\mu$ m wide and deep). Nozzle width 2  $\mu$ m. Sample flow rate  $\approx$  nL/s.

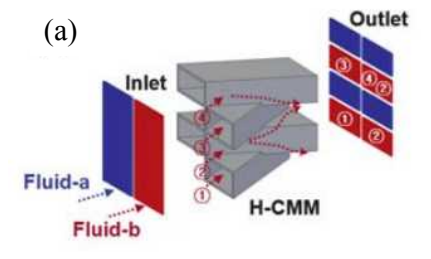
 $"Microfluidics" {\it -- Thomas Lehnert -- EPFL (Lausanne)}$ 

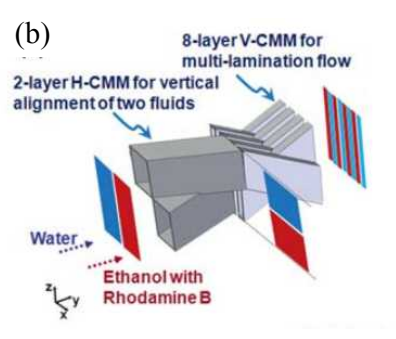


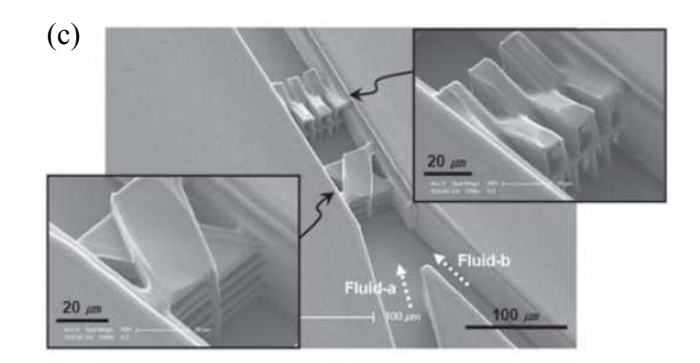
# Example 2: 3D crossing manifold micromixer (CMM)

T.W. Lim et al., Lab Chip, 2011, 11, 100-103

A sequential configuration of horizontally and vertically crossing tube bundles generates and crosses solution lamella for efficient mixing.

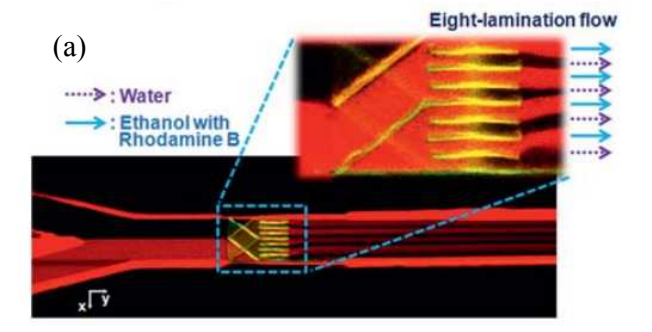




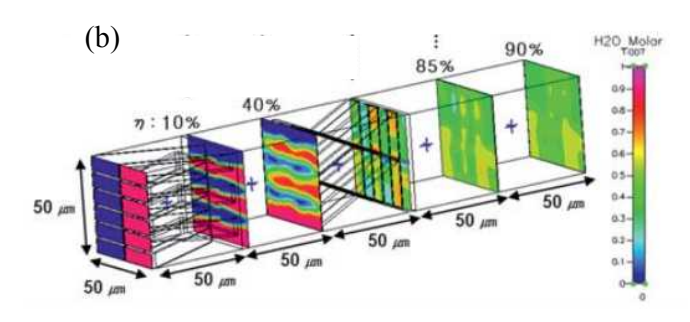


(a) Principle of the horizontally crossing manifold micromixer (H-CMM, 2 layers); (b) horizontally and vertically crossing manifold micromixers (H/V-CMM); (c) SEM images of the H/V-CMM fabricated in the SU8 microchannel by two-photon stereolithography.

(a) Multi-laminar flow with 8 fluid segments is visible after a 2 layer H-CMM and 8 layer V-CMM. Ethanol with rhodamine B (red fluorescence) and water flow from left to right.



(b) Mixing efficiency vs. distance from H/V-CMM of six layers (simulation, Re = 1 and Pe = 1000). The two fluids are split into 36 segments by H/V-CMM and almost completely mixed at 5x the channel width (*i.e.* after 200  $\mu$ m, compared to the several millimetres required in a smooth straight channel.

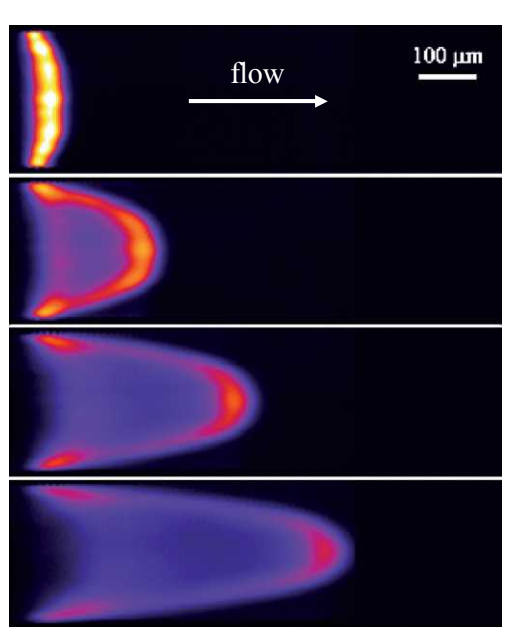


T.W. Lim et al., Lab Chip, 2011, 11, 100–103

"Microfluidics" -- Thomas Lehnert -- EPFL (Lausanne)

# 4.2.4 Taylor dispersion and the rotary mixer





Dispersion of a fluo-dye in a microchannel (250  $\mu$ m x 70  $\mu$ m) in a pressure-driven flow.

P. H. Paul, et al., Anal. Chem. 1998, 70, 2459-2467

S. Devasenathipathy and J. Santiago, Microscale Diagnostic Techniques, Springer, New York, USA, 2005, chap. Electrokinetic Flow Diagnostics, pp. 121–166.

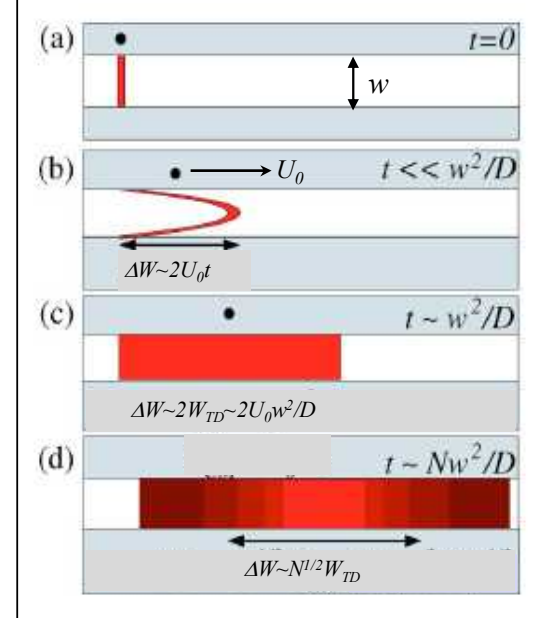
*Initial condition:* A narrow homogeneous band (a plug) of solute(s) is introduce in the channel at t = 0 (e.g. in high-performance liquid chromatography). The initial concentration gradient is in the axial direction.

- ⇒ Upon application of a steady pressure gradient (Poiseuille flow), an initially uniform dye blob is pulled into a parabolic flow "bullet shape".
- ⇒ Convective stretching creates strong **radial gradients**.
- ightharpoonup Diffusion in radial direction tends to homogenize the dye over the channel cross section. Eventually, a dispersed band with no radial concentration gradient moves through the channel at an average speed  $V_0$ .
- ⇒ Due to axial dispersion, band broadening occurs with an effective "Taylor diffusion coefficient" *D*\* that may be much larger than the molecular diffusivity *D* alone (with no flow).

## Taylor dispersion: Intuitive approach



T. M. Squires and S. R. Quake "Microfluidics: Fluid physics at the nanoliter scale" Rev. Mod. Phys., Vol. 77, p.977, 2005



Thin tracer stripe in a channel of width w(t=0).

The stripe is convectively stretched into a parabolic shape. Its width  $\Delta W$  increases linearly with time (center of mass speed  $U_0$ ).

After a characteristic time scale  $\tau_{diff}^{rad} = w^2/D$  for tracers to diffuse across the channel (radially), the parabola is "smoothed".

Each tracer molecule performs N axial random steps  $\Delta W \sim U_0 w^2/D$  as the plug moves on, resulting in a Gaussian distribution of the concentration profile c(x,t) that moves with  $U_0$  in axial direction and spreads with  $\Delta W$ .

 $\Delta W \sim (D^*t)^{0.5} = [(U_0^2 w^2/D)t]^{0.5} \sim Pe~(D \cdot t)^{0.5} \implies D^* \sim Pe^2 D$   $D^*$  is an effective diffusion coefficient enhanced by Talyor dispersion.

"Microfluidics" -- Thomas Lehnert -- EPFL (Lausanne)

# Taylor dispersion derived from the diffusion-convection equation



(for more details see H. Bruus "Theoretical Microfluidics)

Starting with the convection-diffusion eqn (5.22) for a cylindrical microchannel

$$\partial_t c + v_x \partial_x c = D \left( \partial_r^2 c + \frac{1}{r} \partial_r c + \partial_x^2 c \right) \tag{5.49}$$

...the 1D convection-diffusion equation for Taylor dispersion can be written

$$\partial_t \bar{c} + U_0 \, \partial_x \bar{c} = D^* \, \partial_x^2 \bar{c}$$

for  $t >> \tau_{diff}^{rad}$  (when the dye has diffusively spread over the channel cross-section).

 $\hat{c}(x,t)$  is the concentration averaged over the cross-section at x,  $D^*$  is the Taylor dispersion coefficient and  $U_0$  is the average flow speed.

$$\bar{c}(x,t) = \frac{c_0}{\sqrt{(\pi D^* t)}} exp\left[-\frac{(x - U_0 t)^2}{4D^* t}\right]$$
(5.67)

Solution (for  $D^* >> D$ ): The concentration profile evolves as a Gaussian that moves with  $U_0$  in x-direction and spreads  $\sim Pe(D^* \cdot t)^{0.5}$ 



# Axial dispersion coefficients $D^*$ for different geometries

from N.T. Nguyen and S. T. Wereley "Fundamentals and applications of microfluidics", Boston: Artech House, 2006

Cylindrical capillary: diameter d,  $Pe_d = U_0 d/D$ 

$$D^* = D\left[1 + \frac{1}{48}Pe_d^2\right]$$

Two parallel plates: gap *H*,  $Pe_H = U_0 H/D$ 

$$D^* = D \left[ 1 + \frac{1}{210} P e_H^2 \right]$$

Rectangular Channel: width W, height H f(H/W) is a fet of aspect ratio,  $Pe_W = U_0W/D$ 

$$D^* = D \left[ 1 + \frac{1}{210} P e_W^2 f(\frac{H}{W}) \right]$$

 $\Rightarrow$  For high Pe numbers the effective diffusivity D\* increases  $\sim Pe^2$  and becomes much higher than the molecular diffusivity D.

e.g. for a capillary:

for 
$$Pe = 0.1$$
  $D^* \approx D$ 

for 
$$Pe = 100$$

for 
$$Pe = 100$$
  $D^* \approx 2 \cdot 10^{+2} D >> D$ 

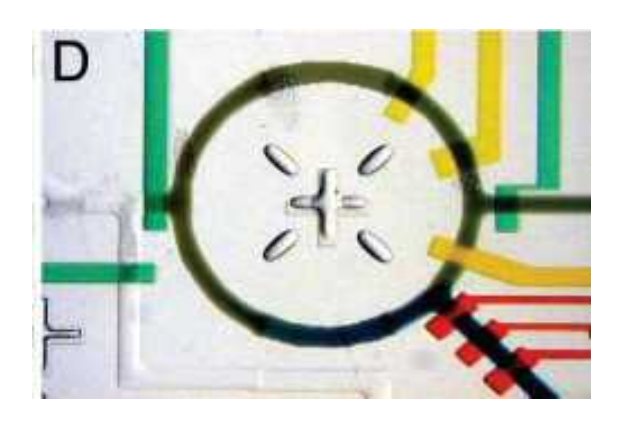
"Microfluidics" -- Thomas Lehnert -- EPFL (Lausanne)

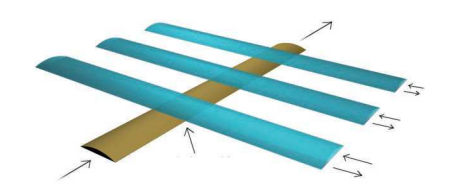
# The rotary mixer

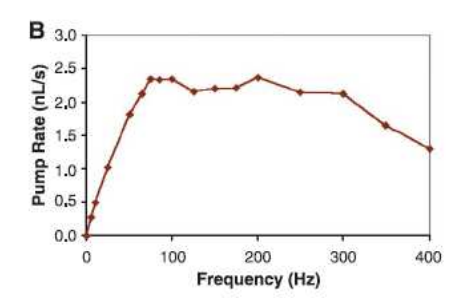
How fast mix the fluids?

R ring diameter, h channel width, mean speed  $U_0$ , D thermal diffusivity,  $D^*$  Taylor diffusivity,  $\tau_D$ diffusion time across the channel width.

$$Pe = rac{ au_D}{ au_{h,conv}} = rac{U_0 h}{D} \qquad {with} \qquad rac{ au_D \sim h^2/D}{and} \qquad au_{h,conv} = h/U_0$$





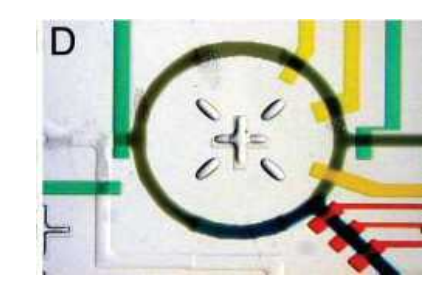


peristaltic pump for integrated microfluidic devices and typical pumping rates (channels are 100 µm wide and 10 µm high).

Marc A. Unger, et al., Science 288, 113 (2000)

T. M. Squires and S. R. Quake: Microfluidics: Fluid physics at the nanoliter scale, Rev. Mod. Phys., Vol. 77, p.977, 2005

$$Pe = rac{ au_D}{ au_{h,conv}} = rac{U_0 h}{D}$$
 with  $au_D \sim h^2/D$  and  $au_{h,conv} = h/U_0$ 



#### 3 mixing regimes:

- **Diffusion dominated** (mixing time  $\tau_R$ )

**Pe** 
$$<<$$
 1, for  $U_0 \rightarrow 0$ ,  $D \approx D^*$ 

Basically only thermal diffusion around the ring.

- *Taylor dispersion mediated* (mixing time  $\tau_{TD}$ ) 1<< Pe <  $2\pi R/h$ 

Diffusion across the channel width occurred before a full convective cycle.

- *Convective stirring* (mixing time  $\tau_{con}$ )

$$Pe >> 2\pi R/h$$

Mixing after multiple cycles before efficient lateral diffusion occurs.

$$\tau_R \sim \frac{(2\pi R)^2}{D} = \left(\frac{2\pi R}{h}\right)^2 \tau_D.$$

$$\tau_{TD} \sim \frac{(2\pi R)^2}{D^*} \sim \frac{D(2\pi R)^2}{U_0^2 h^2} \sim {\rm Pe}^{-2} \tau_R.$$

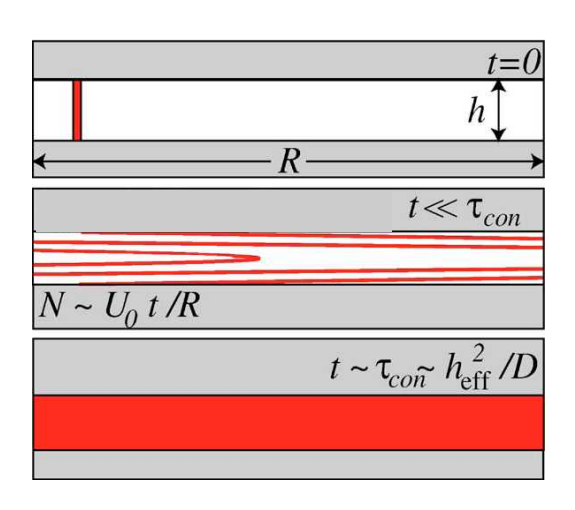
$$N_{\rm con} \sim \left(\frac{h}{\pi R}\right)^{1/3} \text{Pe}^{1/3},$$

$$au_{
m con} \sim {
m Pe}^{-2/3} \left(\frac{\pi R}{h}\right)^{2/3} au_D \sim {
m Pe}^{-2/3} \left(\frac{h}{\pi R}\right)^{4/3} au_R$$

T. M. Squires and S. R. Quake: Microfluidics: Fluid physics at the nanoliter scale, Rev. Mod. Phys., Vol. 77, p.977, 2005

# **EPFL**

# Convective stirred mixing mode (for $Pe >> 2\pi R/h$ )



- An vertical stripe deforms in the parabolic flow. For high *Pe* number lateral diffusion is very slow compared to convection.
- Fluidic elements are stretched linearly in time ( $\sim U_0$ ).
- The effective distance between branches of the stripe reduces to  $h_{\text{eff}} \sim h/2N$  after N cycles.
- ...until, after  $N_{\rm con}$  cycles and a time  $\tau_{\rm con}$ , molecular diffusion across  $h_{\rm eff}$  is fast enough (time  $\tau_{\rm h,eff}$ ) to homogenize the channel, *i.e.*

$$\tau_{\rm con} \approx \tau_{\rm h,eff}$$

$$\tau_{\rm h,eff} = h_{\rm eff}^2/D = (h/2N)^2/D$$
and
$$\tau_{\rm con} = (2\pi R)N_{\rm con}/U_0$$

$$\Rightarrow \qquad \tau_{\rm con} \sim (\pi R/h)^{2/3} P e^{-2/3} \tau_D, \text{ with } \tau_D = h^2/D$$

$$N_{\rm con} = (\tau_{\rm con} U_0)/2\pi R \sim (h/\pi R)^{1/3} P e^{1/3}$$

Rotary mixers are most efficient for batch processes ("bands)" where high gradients are generated by dispersion; not efficient for parallel flow structures.

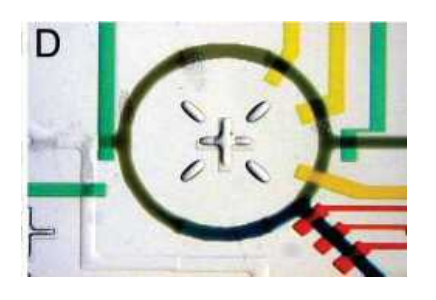
T. M. Squires and S. R. Quake: Microfluidics: Fluid physics at the nanoliter scale, Rev. Mod. Phys., Vol. 77, p.977, 2005

Example: *How fast mix the fluids?* 

R = 1 mmRing diameter: Channel width:  $h = 100 \, \mu m$ 

Thermal diffusivity  $D = 50 \mu m^2/s$  (small protein)

 $\Rightarrow$  Radial diffusion time  $\tau_D \sim h^2/D = 200 \text{ s}$ 



 $Pe \ll 1$ 

$$\tau_R \sim \left(\frac{2\pi R}{h}\right)^2 \tau_D.$$

 $\tau_R \approx 200 \text{ h}$ 

- Taylor dispersion mixing

1 < Pe < 60

$$au_{TD} \sim \mathrm{Pe^{-2}} au_R$$

$$\tau_{TD} \approx 800 \text{ s (for } Pe = 30)$$
  
 $N_{TD} = 2 \text{ cycles, } U_0 = 15 \text{ } \mu\text{m/s}$ 

$$\tau_{TD} = \tau_D \approx 200 \text{ s (for } Pe = 60)$$
  
 $N_{TD} = 1 \text{ cycle, } U_0 = 30 \text{ } \mu\text{m/s}$ 

Pe >> 60

$$au_{\rm con} \sim {
m Pe}^{-2/3} \left( \frac{h}{\pi R} \right)^{4/3} au_R \qquad \begin{array}{l} au_{con} \approx 72 \ {
m s} \ ({
m for} \ Pe = 10^3) \\ N_{con} = 3.2 \ {
m cycles}, \ U_0 = 500 \ {
m \mu m/s} \end{array}$$

$$N_{\rm con} \sim \left(\frac{h}{\pi R}\right)^{1/3} {\rm Pe}^{1/3},$$
  $\tau_{con} \approx 16 {\rm s \ (for \ } Pe = 10^4)}{N_{con} = 6.5 {\rm \ cycles}, \ U_0 = 5 {\rm \ mm/s}}$ 

$$\tau_{con} \approx 72 \text{ s (for } Pe = 10^3)$$

$$N_{con} = 3.2$$
 cycles,  $U_0 = 500$  µm/s

$$\tau_{con} \approx 16 \text{ s (for } Pe = 10^4)$$

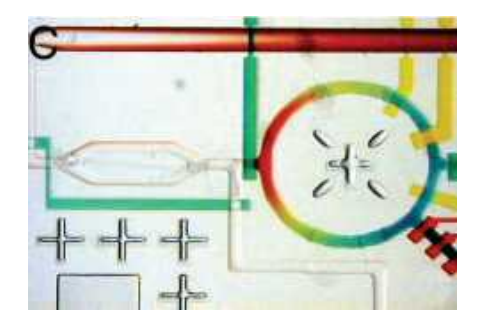
T. M. Squires and S. R. Quake: Microfluidics: Fluid physics at the nanoliter scale, Rev. Mod. Phys., Vol. 77, p.977, 2005

# Application: Protein solubility mapping

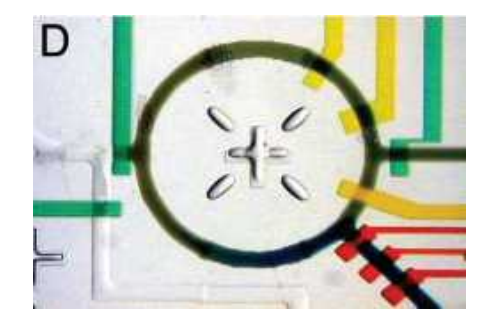
C.L. Hansen et al., PNAS, vol. 101 no. 40 14431–14436 (2004)



- Microfluidic formulation device that allows for the combinatorial mixing of 16 buffers and 16 precipitation agents with a purified protein sample.
- The metering scheme allows for sequential injection of precise sample aliquots (80 pL/cycle).
- $\Rightarrow$  Screening of thousands of different protein solubility conditions with  $\approx \mu L$  of protein sample.

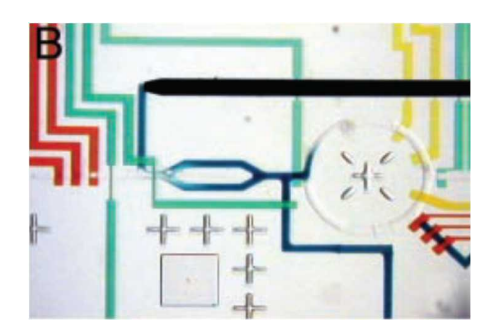


Color gradient formed by consecutive injections into mixing ring. The diameter of the mixing ring is 1.5 mm, volume 5 nL.

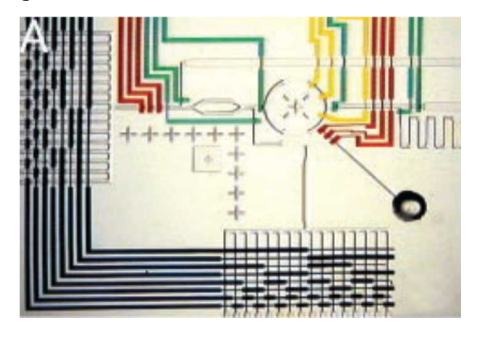


Pumping around ring for 3 sec results in complete mixing of dye. Blue dye is then added to mixture through sample injection inlet (bottom right).

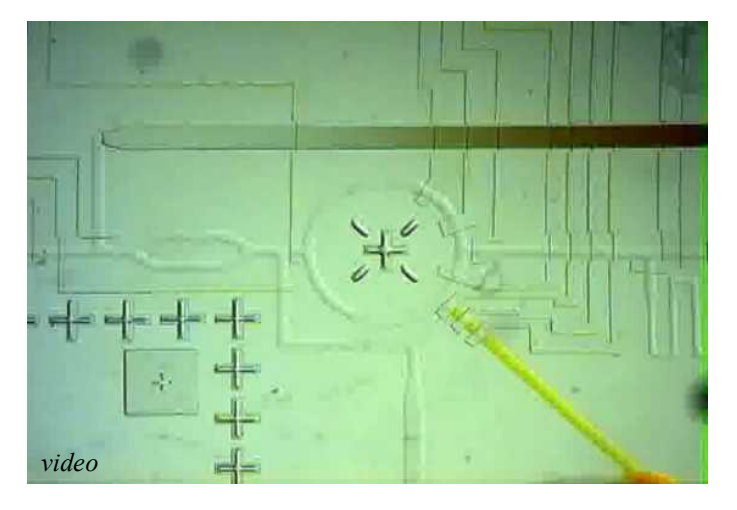
#### Microfluidic formulator for combinatorial mixing on chip (video)



Arbitrary fluid formulations can be mixed on chip by the sequential injection of 80 pL aliquots into a 5 nL microreactor.



Pneumatic control channels for valve actuation.



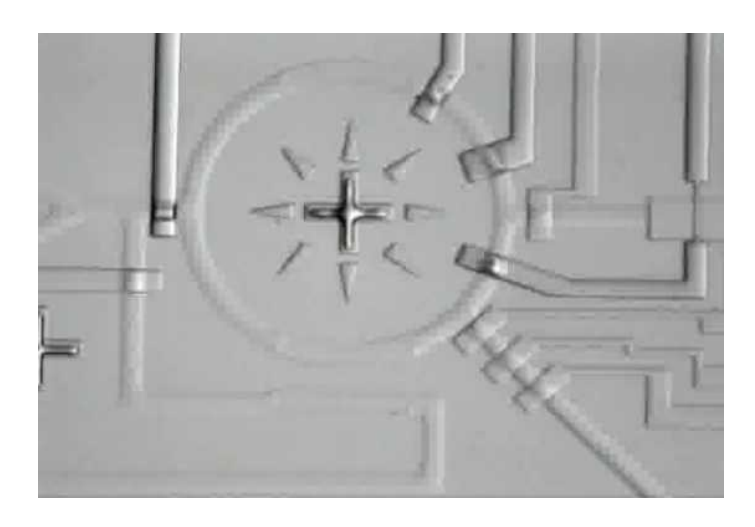
C.L. Hansen et al., PNAS, vol. 101 no. 40 14431-14436 (2004)

Mixer operation: A separate injection port (yellow) is provided for the combination of a precious sample with a large number of unique chemical formulations

Complete mixing of aqueous reagents was achieved in 3 sec (pumps actuated at 100 Hz, flow velocity 2 cm/sec).

# **EPFL**

## Protein solubility mapping using microfluidic formulator (video)



C.L. Hansen et al., PNAS, vol. 101 no. 40 14431-14436 (2004)

Titration of a protein sample (Endo-1,4-b -xylanase) into a 5-nL microreactor in which a precipitating solution (1 M potassium phosphate/0.1 M Tris×HCl) has been mixed.

Precipitation of the protein sample is clearly visible and is detected by using image analysis for fully automated protein phase-space mapping.

# 4.2.5 A multivortex mixer based on inertial flow properties

A.P. Sudarsan and V.M. Ugaz, PNAS, vol. 103(19), 2006, 7228-7233

Mixer based on flow lamination (split-and-recombination) + inertial/centrifugal forces (Dean flow).

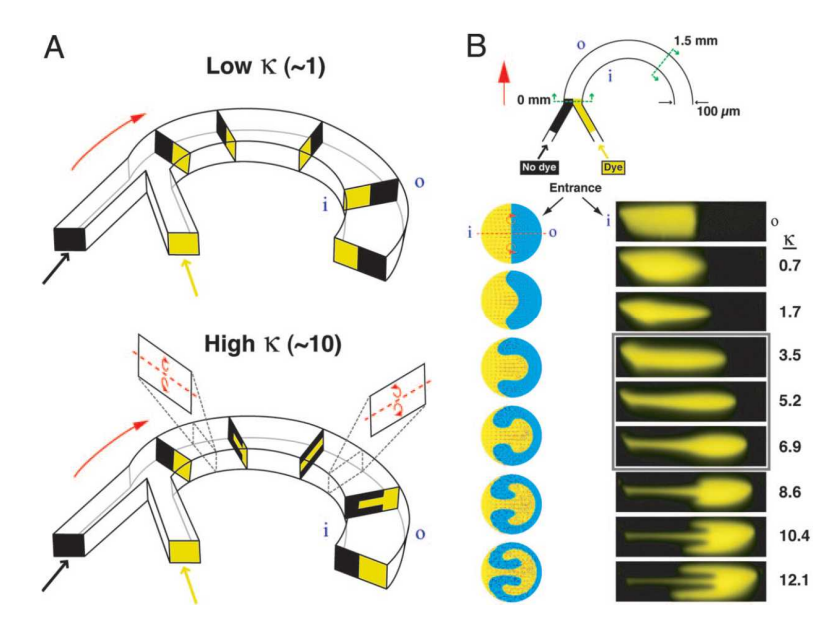
Planar 2D smooth-walled channel geometry generating alternating lamellae of individual fluid species.

**Dean number**  $\kappa$  expresses the relative magnitudes of inertial and centrifugal forces to viscous forces

$$\kappa = \delta^{0.5} Re$$

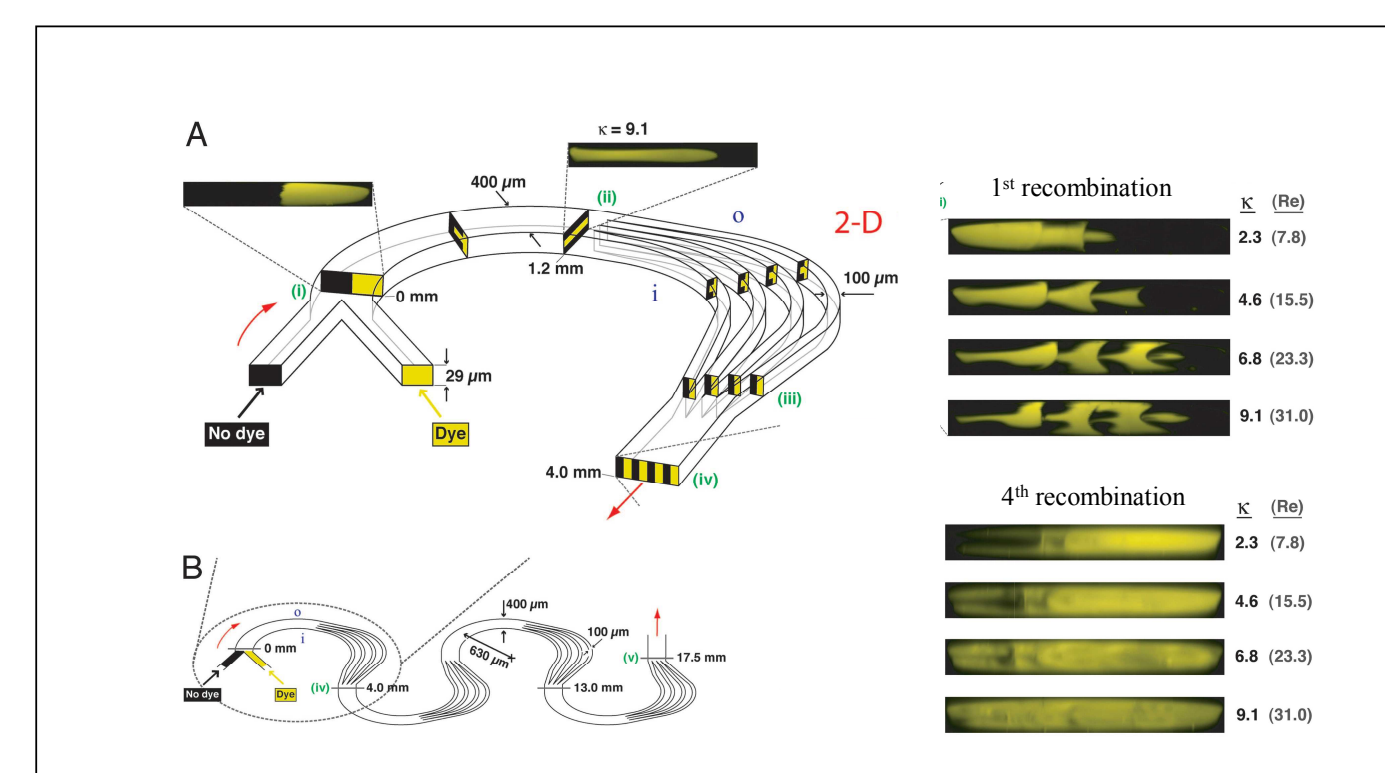
with  $\delta = d/R$ 

R flow path radius of curvature d channel hydraulic diameter



Dean flow in curved microchannels
(100 μm wide; 29 μm tall; 630 μm radius of curvature)

Flow pattern 1.5 mm downstream  $2.6 \le Re \le 45.1 \ (0.7 \le \kappa \le 12.1)$ 



#### Split-and-recombine arrangement for generating alternating lamellae of individual fluid species

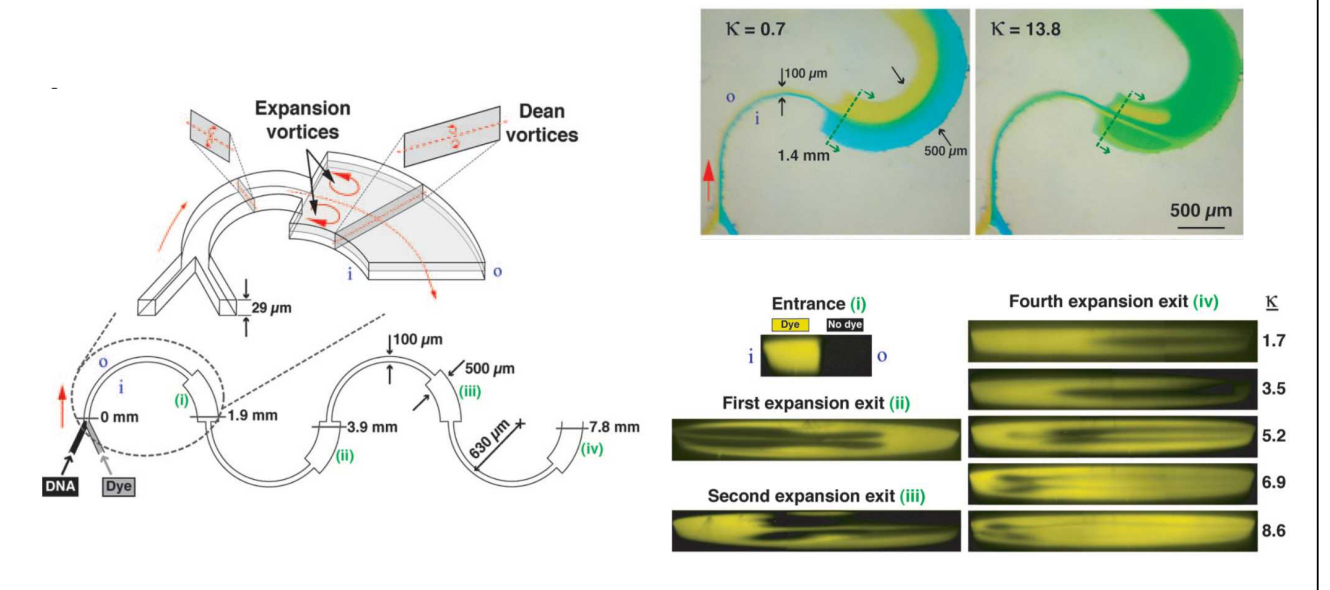
A) (i) Parallel streams enter the curved microchannel and experience a transverse flow generated by the counterrotating vortices; (ii) the flow is split into four parallel streams that proceed along curved trajectories inducing a second pair of  $90^{\circ}$  fluid rotations in each stream (between ii and iii). Alternating lamellae of the two species are generated when the streams are rejoined 4 mm downstream from the entrance (iv).

B) Schematic of a microchannel incorporating a series of successive mixing elements.



Beyond a critical Re, a fluid vortex pair forms at a sudden increase in a conduit's cross-sectional area.

Coupling these expansion phenomena in the horizontal plane with Dean effects in the vertical plane, results in a multivortex flow field that accelerates mixing.



 $6.4 \le Re \le 32.2 (1.7 \le \kappa \le 8.6)$ 

A.P. Sudarsan and V.M. Ugaz, PNAS, vol. 103(19), 2006, 7228-7233

"Microfluidics" -- Thomas Lehnert -- EPFL (Lausanne)

# 4.2.6 Mixing based on chaotic advection



## Chaotic particle trajectories in laminar flow regimes

**Deterministic chaos**: The approximate present does not approximately determine the future, even if the rules are clearly defined.

A dynamic system (deterministic and nonlinear) is defined as *chaotic* if the trajectories of two points (here fluidic elements) diverge exponentially.

$$\delta x(t) \approx \delta x_0 e^{\alpha t}$$
chaotic if  $\alpha > 0$ 

 $\delta x_0$  initial distance of two particles  $\delta x$  is the distance at time t

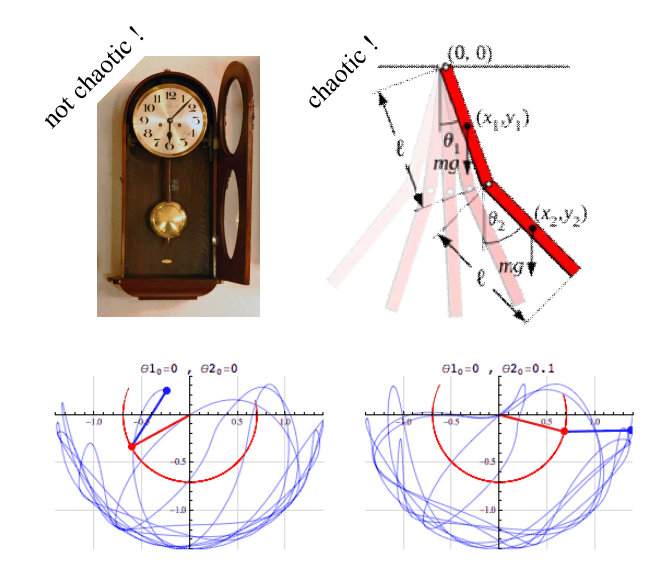
**Lyapunov number**:  $\alpha$  is a parameter that defines the rate of exponential divergence in a chaotic system.

As the trajectories separate at an exponential rate, chaotic systems are extremely sensitive to initial conditions. Experimentally, the initial conditions cannot be defined accurately enough (e.g.  $\delta x_0 \pm \delta x_B$  due to Brownian motion) to predict the particle's position after a certain time t > 0.





Butterfly effect



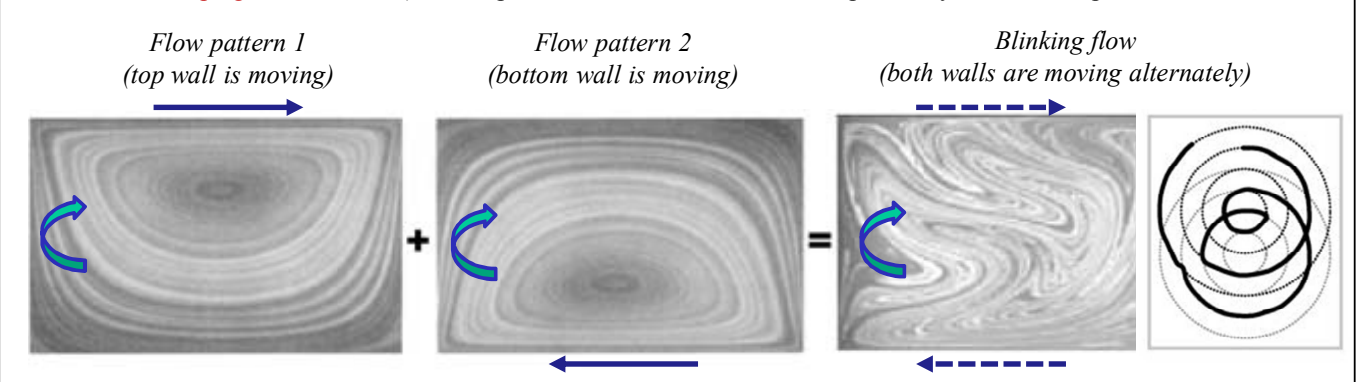
The motion of a double pendulum is governed by a set of coupled ordinary differential equations and is chaotic (deterministic, not random).

"Microfluidics" -- Thomas Lehnert -- EPFL (Lausanne)

# **EPFL**

Is it possible to create chaotic particle trajectories in a laminar flow system ?  $\Rightarrow$  YES!

**Blinking flow** in a rectangular (macroscopic) cavity (10 x 6 cm<sup>2</sup>, fluorescent dye in glycerine,  $D = 10^{-8}$  cm/s<sup>2</sup>, Re = 1.7, creeping flow condition). The top/bottom wall can be moved independently at constant speed.



One wall (top or bottom) is moving: Initial dye blobs are stretched and follow the streamlines, no mixing. Top/bottom walls move in opposite direction, thus the flow rotation is the same in both cases, but the center of rotation is displaced.

*Picture on the right*: Periodically changing boundary conditions (both walls move alternately), resulting in chaotic and diverging dye trajectories (whereas the streamlines are well-defined).

- ⇒ Very thin striations, high local gradients and exponential decrease of the interface distances may significantly increase diffusive exchange (diffusive mixing).
  - J. M. Ottino, 1989, The Kinematics of Mixing: Stretching, Chaos, and Transport, Cambridge University Press, Cambridge, England.

## The baker's transformation and chaotic mixing





cut and fold

**Baker's Transformation:** A given fluidic volume (flow stream) is subjected to *N* cycles of repeated stretching and folding (or cutting and piling up as shown here).

The distance in x direction of two arbitrary points in a layer increases as

$$\delta x(t) \approx \, \delta x_0 \, 2^N {\sim} \, e^{N \, ln2}$$

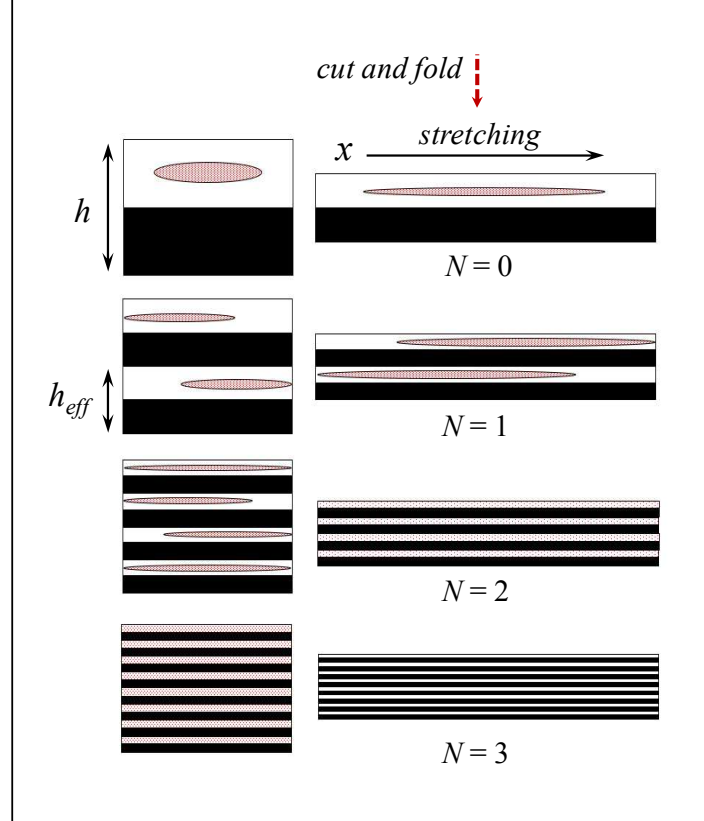
 $\Rightarrow$  A baker's transformation is a process generating deterministic chaos with a Lyapunov exponent  $\alpha = \ln 2$ .

A microfluidic mixer based on Baker's transformation is built up from *N* successive units that perform successive stretching/forlding processes in a continuous flow mode.

 $h \downarrow \qquad \qquad x \underline{\qquad stretching} \\ N = 0 \\ h_{eff} \downarrow \qquad \qquad N = 1$ 

"Microfluidics" -- Thomas Lehnert -- EPFL (Lausanne)

# **EPFL**



The spacing between two layers (or the layer thickness), and *i.e.* the effective diffusion time between two adjacent layers, decreases exponentially with *N* as

$$h_{eff} = \frac{h}{2^N} \sim e^{-N}$$

The fluidic interface, and consequently diffusive mass flow, between two adjacent layers at the mixer inlet also increases exponentially through successive sequences of Baker's transformations.

These facts are used in microfluidic mixers based on *chaotic advection*, resulting in a very efficient mixing process.



# Evaluation of the mixing time / mixing length for a microfluidic mixer based on chaotic advection:

The mixer performs N cycles of a baker's transformation. The time  $\tau_{cyc}$  required per cycle is:

$$\tau_{cyc} = \frac{NL_{cyc}}{U}$$



 $L_{cyc}$ 

 $L_{mix}$ 

where  $L_{cyc}$  is the geometrical length of one cycle structure in the channel (width h) and U is the mean flow velocity in the axial flow direction. After N cycles the fluidic layers are separated by  $h_{eff}$  and the diffusion time  $\tau_{D,eff}$  between adjacent layers becomes

$$\tau_{D,eff} = \frac{h_{eff}^2}{D} = \left(\frac{h}{2^N}\right)^2 \frac{1}{D} = 2^{-2N} \tau_D$$

Full mixing in the channel occurred when  $\tau_{cyc} = \tau_{D,eff}$ , i.e. after  $N_{chaotic}$  cycles or a channel length  $L_{mix}$  which can be expressed as a function of the Pe number (Pe = hU/D)

$$N_{chaotic} \sim \ln Pe$$

$$L_{\text{mix}} = N_{\text{chaotic}} \cdot L_{\text{cyc}} \sim \ln Pe$$

 $\Rightarrow$  much shorter than in a merely diffusion-based mixing process in a linear channel  $(L_{mix} \sim Pe)$ .

Corresponding mixing time  $\tau_{chaotic}$ 

$$au_{chaotic} \sim rac{L_{cyc}}{h} rac{\ln Pe}{Pe} au_D$$

T. M. Squires and S. R. Quake: Microfluidics: Fluid physics at the nanoliter scale, Rev. Mod. Phys., Vol. 77, p.977, 2005

# Example 1: Topologic mixing on a microfluidic chip

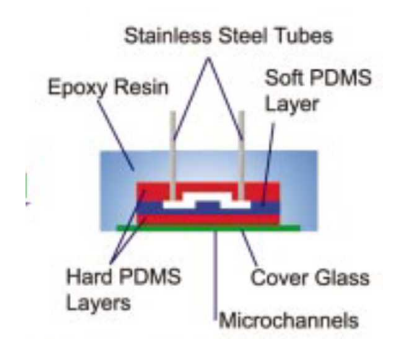


H. Chen, et al., Applied Physics Letters, 2004, Vol. 84, 2193–2195

Topological structure that exploits the laminarity of the flow to repeatedly fold the flow and double the lateral concentration gradient. Lamination increases the interfacial area  $\sim 2^N$ , and reduces the distance between the layers as  $h_{eff} \sim h/2^N$  after N cycles.

The mixer performs a series of Baker's transformations on the concentration profile.

#### ⇒ Chaotic advection



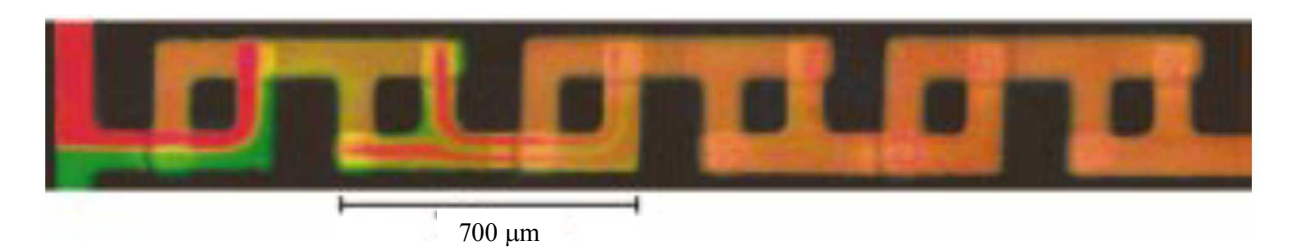
Simplified design eliminating the straight out-of-plane runs.



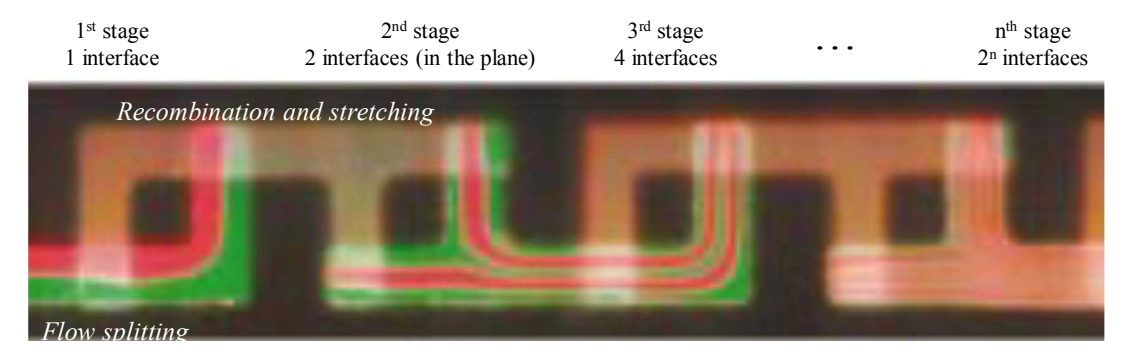
Two identical streams are split and rotated in opposite directions in each channel (width  $100~\mu m$ ). Upon recombination the concentration pattern and gradients are doubled.



A Möbius band-like fluidic flow pattern is generated.



Mixing of two fluorescently labeled protein solutions in a six-stage mixer. The fluids are combined in the T-junction (one sharp boundary layer). After the first two mixing stages, four interfaces, now broadened by diffusion. After 3 stages or a device length of 1.2 mm, the liquids are well mixed (Re = 0.1 and Pe = 0.69).



In the lower micrograph a ten-fold higher viscosity and flow rate was used (*Re* maintained) resulting in mixing after 5 stages (for purely diffusive mixing in a linear channel the mixing length would increase hundred-fold!

"Microfluidics" -- Thomas Lehnert -- EPFL (Lausanne)

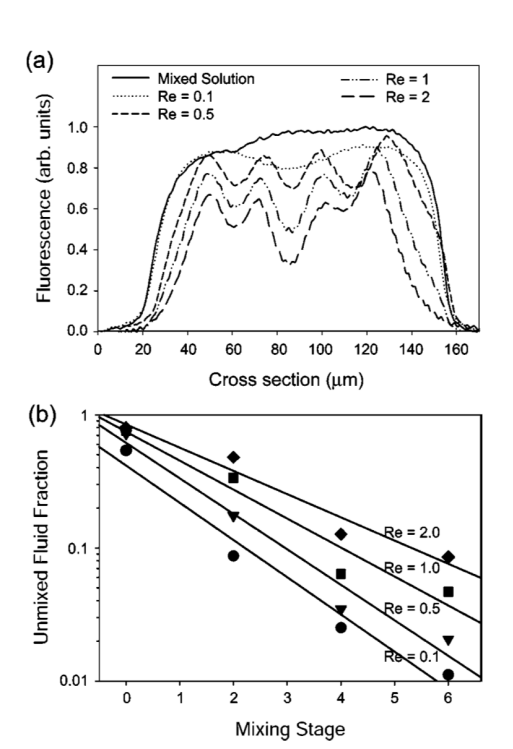
# **EPFL**

#### Is this mixing process based on chaotic advection?

- a) Fluorescence across the flow channel **after two mixing stages**. A Ca<sup>2+</sup>-sensitive dye is mixed with a CaCl<sub>2</sub> solution at different flow velocities. The fluorescence of a premixed solution is shown for comparison. *Re* ranging from 0.1 to 2.
- b) Fraction of unmixed fluid at each stage of the mixer for different flow rates, as determined from the fluorescence measurements.

Linear regression lines in the semilogarithmic display indicate that the unmixed volume indeed decreases exponentially with the number of mixing stages, or equivalently, channel length.

⇒ Even in case of a highly regular flow pattern chaotic advection can be achieved.



H. Chen, et al., Applied Physics Letters, 2004, Vol. 84, 2193–2195

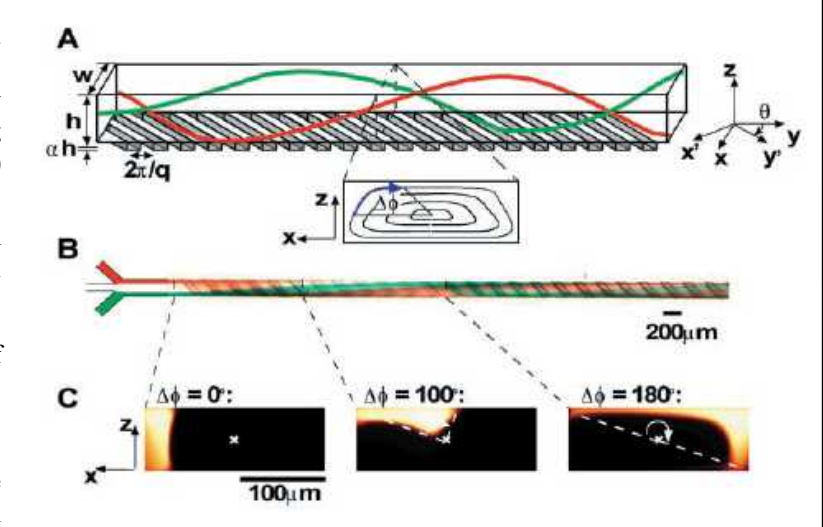
## Example 2: Staggered herringbone mixer (SHM)



A.D. Strook et al., Science, 295, p.647 (2002)

Passive mixing of steady pressure-driven flows in microchannels at low Re numbers ( $0 \le Re \le 100$ ) and high Pe numbers ( $\sim 10^5$ ).

- A) PDMS channel with obliquely oriented ridges on the bottom. A steady axial pressure gradient in y-direction generates a **secondary transverse flow** resulting in 3D twisting trajectories. **Helical streamlines** in the (x,z) cross section are shown.
- B) Top view of a red and a green stream flowing on either side of a clear central stream at the inlet.
- C) Fluorescent confocal micrographs of vertical (x,z) cross sections of the microchannel. The frames show the rotation, distortion and stretching of a fluidic volume element that was injected along one side (fluorescein-labeled polymer in glycerol/water).



Channel ( $h = 70 \mu \text{m}$ ,  $w = 200 \mu \text{m}$ )

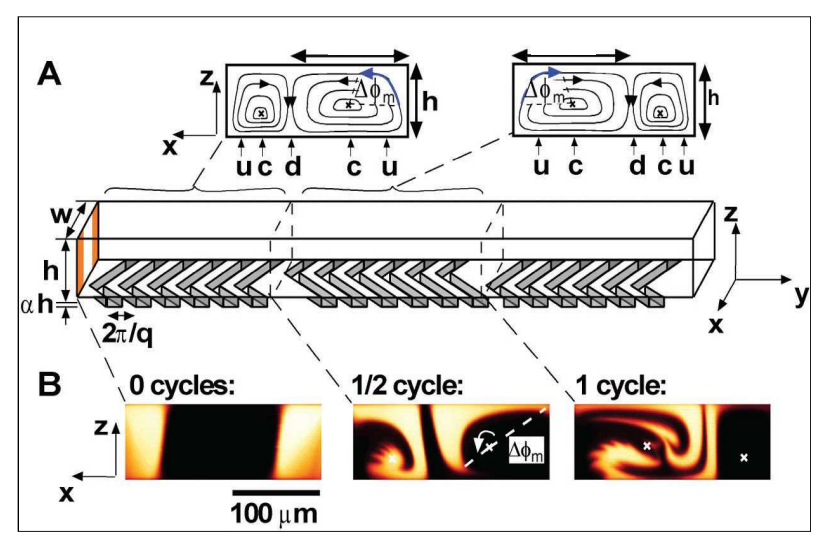
"Microfluidics" -- Thomas Lehnert -- EPFL (Lausanne)

# **EPFL**

#### Staggered herringbone structure

Changing the asymmetry of the herringbone structure after each half-cycle shifts the center of rotation of both secondary flows. Two counter-rotating transverse flows are generated.

⇒ This process corresponds to a **baker's transformation** with repeated folding and stretching of the transverse flows ("blinking flow").



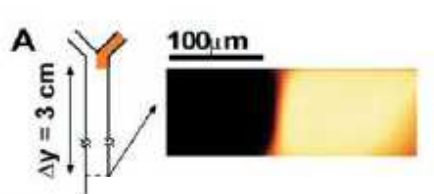
- (A) One-and-a-half cycles of the SHM: One mixing cycle is composed of two sequential regions of ridges with different directions of asymmetry. The streamlines are shown.
- (B) Confocal micrographs cross sections. Two fluorescent solutions were injected on either side of a clear central stream.

Re < 10<sup>-2</sup> h = 77 μm, w = 200 μm, a = 0.23 10 ridges/half cycle  $\rightarrow \Delta \Phi_{\rm m} = 180^{\circ}$ 

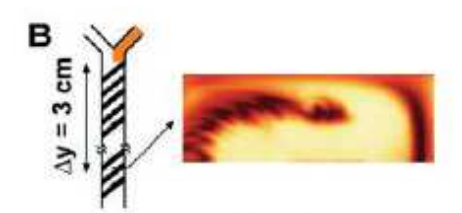
A.D. Strook et al., Science, 295, p.647 (2002)



Two distinct streams at the inlet, mixed at low Re numbers and high Pe numbers All channels: length  $\Delta y = 3$  cm, w = 200 µm, h = 80 µm,  $Re \sim 10^{-2}$ 

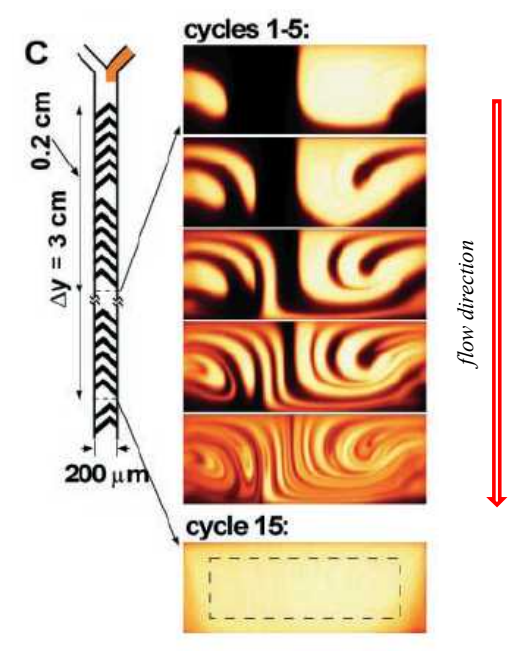


smooth channel walls  $Pe = 2 \times 10^5$ , no mixing



straight grooves on one side  $Pe = 2 \times 10^5$ , incomplete mixing

A.D. Strook et al., Science, 295, p.647 (2002)



SHM,  $Pe = 9 \times 10^5$  (!)  $\Rightarrow$  full mixing

The distance between two stripes, i.e. the effective diffusion length, decreases  $\sim 2^{-N}$  after N cycles.

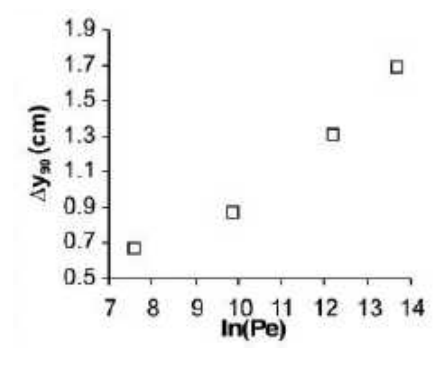
# EPFL

The mixing length  $y_m$  grows only logarithmically with the Pe, as expected for mixing based on chaotic advection:

#### SHM $\Delta y_{90\%} \sim \ln Pe$

For comparision: Mixing length  $y_m$  for purely diffusive in a straight channel with smooth walls ( $U_0$  mean flow speed):

$$\Delta y_m \sim U_0(w^2/D) = Pe \cdot w$$



increase with ln*Pe* experimental mixing (90%) length in a SHM structure (for  $Pe = 2 \times 10^3$  to  $9 \times 10^5$ ).

Example: Mixing of a proteins in aqueous solution

$$D \approx 10^{-6} \, \text{cm}^2/\text{s}$$
,  $w = 100 \, \mu\text{m}$ 

with 
$$U_0 = 1 \text{ cm/s}, Pe = 10^4$$

$$U_0 = 10 \text{ cm/s}, Pe = 10$$

Smooth walls

$$\Delta y_m \sim 100 \text{ cm}$$

$$\Delta y_m \sim 10 \text{ m (!)}$$

SHM

$$\Delta y_m \sim 1 \text{ cm}$$

$$\Delta y_m \sim 1.5 \text{ cm}$$

A.D. Strook et al., Science, 295, p.647 (2002)